were immersed in a graduated series of sucrose solutions (20 ~ 40 % w/v) in PBS at 4°C, embedded in Tissue-Tek Oct Compound (Miles Laboratory, Elkhart, IN, USA), and frozen. Middle portions of the muscles were cut at a 10 μm thickness by a cryostat and air-dried for 1 h at room temperature. The sections were stained by hematoxylin and eosin, and observed under a light microscope. The total and degenerative areas of the muscles on the sections were measured using an image analyzer (Luzex 3U; Nikon, Tokyo, Japan). The degenerative area was normalized by the total area and expressed as a percent value of the total area of the muscles.

Immunohistochemistry for m-cadherin and utrophin. To detect the satellite cells in the mdx and B10 muscles, the cryosections of the muscles were immunostained for a goat antibody against m-cadherin (Santa Cruz Biotechnology Inc., Santa Cruz, CA, USA) as described previously (31). The number of m-cadherin-positive cells in the periphery of myofibers and in the degenerative area was counted as satellite cells in a total of 10 rectangular areas of 140 X 130 μm^2 on several sections obtained from each mouse (21). The 10 rectangular areas, which were not overlapped and were uniformly distributed on the sectional area of muscles, were selected throughout the several sections and were approximately 5 ~ 20% of total sectional areas of the B10 and mdx muscles. The number of total cell nuclei in muscle tissues was also counted and the percentage of m-cadherin-positive cells to the total number of cell nuclei in the muscle tissues was calculated. The percentage values in the 10 rectangular areas were averaged to obtain the mean value for each mouse. This mean value was further averaged to obtain the mean value for six mdx or six B10 mice. To analyze the change in the expression of utrophin, immunostaining for utrophin was performed using a goat antibody against utrophin (Santa Cruz Biotechnology Inc., Santa Cruz, CA, USA). For control staining, the primary antibody was replaced with PBS or normal goat IgG.

RNA extraction, reverse transcription, and competitive-polymerase chain reaction (competitive PCR) amplification. Six mdx and six B10 mice, aged 6 weeks, were killed by cervical dislocation under ether anesthesia. The body weights of the mdx and B10 mice were 19.8 ± 0.8 g and 24.3 ± 0.5 g (mean ± 1 SD), respectively. Whole portions of the left masseter, gastrocnemius, soleus, and diaphragm muscles were removed, immediately frozen, and stored at -80°C until use.

Total RNA extraction, reverse transcription, and competitive-PCR amplification were performed as previously described (34, 36). Briefly, total RNA extraction was performed according to the manufacturer's specifications (Rapid Total RNA Isolation Kit; 5 Prime→3 Prime Inc., Boulder, CO, USA). The RNA was treated with 2 units of ribonuclease-free deoxyribonuclease I (Life Technologies, Gaithersburg, MD, USA), and was then reverse transcribed with 200 units of reverse transcriptase (SuperScript II; Life Technologies, Gaithersburg, MD, USA).

In the conventional PCR technique, a small difference in the starting amount of target DNA can result in a large change in the yield of the final product due to the exponential nature of the PCR reaction. A plateau effect after many cycles can lead to an inaccurate estimation of final product yield. Furthermore, since the PCR amplification depends on the reaction efficiency, small changes in the efficiency can lead to major differences in the final product yield. To overcome these problems, the competitor (internal standard), which has the same primer sequences as those of the target DNA at the 5' and 3' ends, was amplified simultaneously with the target (10, 25, 34, 36). Competitors for the competitive-PCR amplification were constructed according to the manufacturer's instructions (Competitive DNA Construction Kit; Takara, Shiga, Japan). The sequences of primers for pax7, m-cadherin, and utrophin were as follows: pax7, 5'-CCA CAG CTT CTC CAG CTA CTC TG-3' and 5'-

CAC TCG GGT TGC TAA GGA TGC TC-3' (29); m-cadherin, 5'-ATG TGC CAC AGC CAC ATC G-3' and 5'-YCC ATA CAT GCT CGC CAG C-3' (13); utrophin, 5'-AAA CTC CTA TCA CGC TCA TCA-3' and 5'-CTC ATC CTC CAC GCT TCC T-3' (8). Those for S16 were identical to those used in our previous report (17). The amplification products were isolated by electrophoresis on an agarose gel containing ethidium bromide. The fluorescent intensities of the bands of the target genes (upper bands in Fig. 1A) and their respective competitors (lower band in Fig. 1A) were measured by an image analyzer (Molecular Imager FX; Bio-Rad, Hercules, CA, USA). We then calculated the ratios of the fluorescent intensities of the target gene bands to those of their respective competitors. The logarithmic value of the fluorescent intensity ratio was used to calculate the amount of endogenous target mRNA based on the line formula derived from a standard curve for each target gene. The standard curve was generated as described previously (17, 35). Fig. 1B shows the standard curve for m-cadherin calculated by using the image analysis data of electrophoretic bands, as shown in Fig. 1A. The slope of the regression line was 0.772 and the correlation coefficient was 0.994, which was significantly different from zero ($p<0.001$). The quantity of each target gene was normalized by the quantity of S16 (ribosomal protein). The resulting ratio value in each sample was expressed as a percent value relative to the mean value for the B10 masseter muscle. Since each percent value relative to the mean value for the B10 masseter muscle (% of B10 masseter value) was an arbitrary unit, it was used in the scatter diagrams of Figs. 3, 4 and 5, although there was no data on the B10 muscles in the scatter diagrams.

Statistical Analyses. Tukey-Kramer's method was used to compare multiple combinations of 2 muscles among the 4 mdx muscles. Student's t-test was used to compare single combination of the same types of muscles between the B10 and mdx mice. Regression analysis was used to examine the correlations in the mdx mice between the degenerative areas

of the skeletal muscles and the expression levels for pax7 or utrophin mRNA, and between the degenerative areas of the skeletal muscles and the percentages of m-cadherin-positive cells to the total number of cell nuclei in the muscle tissues. Differences were considered significant at $p< 0.05$.

RESULTS

To detect the degenerative area of the mdx muscle, cryosections from the middle portions of the muscles were stained by hematoxylin and eosin (Fig. 2A ~ 2D). In the mdx gastrocnemius and diaphragm muscles, histopathological changes such as myofiber degeneration (Fig. 2B, 2D) were observed. By contrast, none of the muscles of the control B10 mice showed such histopathological changes (data not shown). Figure 2E compares the degenerative area relative to the total cross sectional area of the mdx muscles. The degenerative areas of the diaphragm and gastrocnemius muscles were $11.7 \pm 3.6\%$ and $8.5 \pm 3.7\%$ of the total muscle areas, respectively. They were significantly greater than those of the masseter ($2.8 \pm 1.6\%$) and soleus ($2.4 \pm 1.5\%$) muscles ($p<0.01 \sim p<0.001$).

To determine whether muscle satellite cells are correlated with the degree of damage in mdx skeletal muscles, we analyzed the expression of pax7 (Fig. 3) and m-cadherin (Fig. 4), which are both markers for muscle satellite cells. Figure 3A shows a typical example of a gel electrophoretic pattern of pax7 competitive PCR products for the masseter, gastrocnemius, soleus, and diaphragm muscles of the B10 mice. The fluorescent intensities of the pax7 bands (lower band) and of its respective competitor bands (upper band) were measured by an image analyzer. The image analyses of the PCR bands indicated that, in all the muscles studied except for the gastrocnemius muscle, the expression levels for pax7 mRNA were significantly higher in the mdx than in the B10 mice ($p<0.05 \sim 0.01$, Fig. 3B). In the mdx mice, the expression level for pax7 mRNA in the masseter muscle was more than 6-fold higher than those in the

soleus and diaphragm muscles ($p<0.01$), but was not significantly different from that in the gastrocnemius muscle. Figure 3C shows a scatter diagram and a regression line between the degenerative areas of the skeletal muscles and the expression levels for pax7 in the mdx mice. The correlation coefficient was -0.140, which was not significantly different from zero.

In all muscles studied, the mean values of the expression levels for m-cadherin mRNA were higher in the mdx mice than in the B10 mice; only the 2.4-fold increase in the diaphragm muscle was statistically significant (Fig. 4A). In the mdx mice, no significant difference in the expression levels for m-cadherin mRNA was found among the muscles. Since m-cadherin is reportedly expressed in neural cells within muscle tissues (18), we also investigated the immunolocalization of m-cadherin. The number of m-cadherin-positive cells in the periphery of myofibers (the arrow in Fig. 4B) and in the degenerative area (the arrows in Fig. 4C) was counted as satellite cells. M-cadherin-positive cells in the area interspaced among myofibers (the arrows in Fig. 4D) were excluded from the counting. In all the muscles studied except for the gastrocnemius muscle, the percentage of satellite cells to the total number of cell nuclei in the muscle tissues was significantly higher in the mdx than in the B10 mice ($p<0.05 \sim 0.001$, Fig. 4E). In the mdx mice, the percentage of satellite cells to the total number of cell nuclei in the muscle tissues in the masseter muscle was 2.7 ~ 5.4-fold greater than those in the other three muscles ($p<0.01$). The correlation coefficient between the degenerative areas of the skeletal muscles and the percentages of m-cadherin-positive cells to the total number of cell nuclei in the muscle tissues in the mdx mice was -0.411, which was not significantly different from zero (Fig. 4F).

To investigate the relationship between utrophin expression and the degree of damage in the mdx skeletal muscles, we analyzed the expression levels for utrophin mRNA and the immunolocalization of utrophin (Fig. 5). In all muscles studied, the mean values of the expression levels for utrophin mRNA were higher in the mdx than in the B10 mice, and the

1.4- and 3.0-fold increases in the soleus and diaphragm muscles, respectively, were statistically significant ($p<0.05$ and $p<0.001$) (Fig. 5A). In the mdx mice, the expression level for utrophin mRNA in the diaphragm muscle was 1.4 ~ 2.7-fold ($p<0.05 \sim 0.01$) higher than those in the other three muscles and that in the gastrocnemius muscle was approximately 2-fold ($p<0.01$) higher than those in the masseter and soleus muscles. The correlation coefficient between the degenerative areas of the skeletal muscles and the expression levels for utrophin mRNA in the mdx mice was 0.231, which was not significantly different from zero (Fig. 5B). In the B10 mice, immunostaining for utrophin was sporadically found in the periphery of myofibers (black arrowheads in Fig. 5C, 5E). In the mdx masseter muscle, the periphery (black arrowheads) and whole sarcoplasm of regenerative myofibers with central nuclei were immunostained for utrophin (Fig. 5D). The periphery of normal masseter myofibers without central nuclei (white arrowheads) was slightly stained, but the sarcoplasm (arrows) was not stained (Fig. 5D). In the mdx diaphragm muscle, immunostaining for utrophin was observed in both the whole sarcoplasm and periphery of normal and degenerative myofibers, and the immunostaining in the periphery (sarcolemma) of myofibers (black arrowheads) was more intense than that in the sarcoplasm (Fig. 5F). The immunostaining patterns for utrophin in the gastrocnemius and soleus muscles were similar to those in the masseter muscle (data not shown).

DISCUSSION

In the course of skeletal muscle regeneration, quiescent satellite cells are activated to proliferate and, after several rounds of proliferation, the majority of satellite cells differentiates and fuses to form new myofibers or to repair damaged myofibers. We analyzed the expression of pax7 and m-cadherin as markers for satellite cells. Based on their expression patterns and functions (4, 12, 14, 24), pax7 and m-cadherin are considered as markers for quiescent, activating, and proliferating satellite cells. In the present study, the expression level for pax7

mRNA and the percentage of m-cadherin-positive cells to the total number of cell nuclei in the muscle tissues in all four muscles studied were greater in the mdx mice than the in the B10 mice (Fig. 3B, Fig. 4E), suggesting that the activation and proliferation processes of muscle satellite cells occur more actively in mdx muscles than in B10 muscles. Reimann and his co-workers reported no significant difference in the percentage of m-cadherin-positive cells to the total number of cell nuclei in the soleus muscle between B10 and mdx mice, which appears to be inconsistent with our present data. This inconsistency is probably due to the difference in the age of mice between our present study (6 weeks of age) and the study of Reimann et al. (11~14.5 months of age) (21).

In the mdx mice we found no significant correlation between the muscle damage and the expression level for pax7 (Fig. 3C), and none between the muscle damage and the percentage of satellite cells to the total number of cell nuclei in the muscle tissues (Fig. 4F), suggesting that the levels of activation and proliferation of muscle satellite cells are not correlated to the degree of damage in mdx skeletal muscles. However, since the correlation between the muscle damage and the percentage of satellite cells to the total number of cell nuclei in the muscle tissues was nearly significant (when the t value for the correlation is more than 2.07, it indicates that the correlation is statistically significant and t value in the present result was 2.01), muscle satellite cell seems to be one of several factors for influencing the degree of damage in mdx skeletal muscles, but not a great influencing factor. Gillis proposed the following three factors that can lead to severe myofiber damage in the mdx diaphragm muscle (11): i) a large proportion of fast oxidative fibers having a large diameter, ii) a life-long sustained activity, and iii) forced lengthening during each contraction. Further studies are necessary to elucidate the factors that determine the degree of damage in mdx skeletal muscles other than the diaphragm muscle.

In both the B10 and mdx mice, the percentages of m-cadherin-positive cells to the total number of cell nuclei in the muscle tissues were greatest in the masseter muscles. This result indicates that the masseter muscle contains a largest pool of satellite cells, suggesting that the regeneration potential of the masseter muscle is much larger than those of the other muscles. If the same situation exists in the mdx muscles prior to the first episode of degeneration, it would not be surprising that the mdx masseter muscle showed much less damage than the mdx diaphragm muscle (Fig. 2E). In the present study, however, clear and statistically-significant negative correlation between the muscle damage and the percentage of satellite cells can not be obtained (Fig. 4F). This is probably due to the existence of more influencing factors than satellite cells. Masseter muscle reportedly has the several unique characteristics relative to other muscles (3, 5, 16, 26, 28, 32), and to these we may now add the characteristic of having a large pool of satellite cells and large potential of regeneration.

Previous studies have reported that utrophin can functionally replace dystrophin and that the transgene expression of utrophin can prevent muscular dystrophy in mdx mice (2, 7, 30). Thus, we had expected a high negative correlation between damage to the skeletal muscles and the expression level for utrophin mRNA in the mdx mice. Contrary to our expectation, the correlation coefficient between the muscle damage and the expression level was low and not significantly different from zero (Fig. 5B). In particular, the mdx diaphragm muscle exhibited the highest expression level for utrophin mRNA, although it was the most severely damaged by dystrophy. To determine whether the up-regulated utrophin can not functionally replace dystrophin, because it is not incorporated into the sarcolemma instead of dystrophin, we investigated the immunolocalization of utrophin (Fig. 5C ~ 5F). Since intense immunostaining for utrophin was observed in the periphery of mdx myofibers (Fig. 5D, 5F), we presumed it was incorporated into the sarcolemma. In the present study, the expression level for utrophin mRNA in the mdx diaphragm muscle was 1.4 ~ 2.7-fold higher than those in

the other three mdx muscles studied (Fig. 5A). To obtain a complete disappearance of muscle damage, transgene expression is needed to reach approximately 11-fold and 25-fold higher than the utrophin expressions in the mdx and normal mice, respectively (22). Thus, it is most likely that the difference in the spontaneous up-regulation of utrophin among different mdx muscles is too small to produce a difference in the degree of damage among different mdx muscles.

We would like to thank Professor M. Chiba, Tsurumi University School of Dental Medicine, for his support throughout the present study.

This study was supported in part by grants-in-aid for funding scientific research (No. 13671955, No. 16591871 to A.Y.), the Bio-ventures and High-Technology Research Center from the Ministry of Education, Culture, Sports, Science, and Technology of Japan, and by the Science Research Promotion Fund from the Promotion and Mutual Aid Corporation for Private Schools of Japan.

REFERENCES

1. Adams GR. Role of insulin-like growth factor-I in the regulation of skeletal muscle adaptation to increased loading. Exerc Sport Sci Rev 26: 31-60, 1998.
2. Blake DJ, Weir A, Newey SE, and Davies KE. Function and genetics of dystrophin and dystrophin-related proteins in muscle. Physiol Rev 82: 291-329, 2002.
3. Butler-Browne GS, Eriksson P-O, Laurent C, and Thornell L-E. Adult human masseter muscle fibers express myosin isozymes characterisitic of development. Muscle Nerve 11: 610-620, 1988.
4. Charge SBP and Rudnicki MA. Cellular and molecular regulation of muscle regeneration. Physiol Rev 84: 209-238, 2004.
5. d'Albis A, Janmot C, and Bechet J-J. Comparison of myosins from the masseter muscle of adult rat, mouse and guinea-pig. Persistence of neonatal-type isoforms in the murine muscle. Eur J Biochem 156: 291-296, 1986.
6. Deconinck AE, Rafael JA, Skinner JA, Brown SC, Potter AC, Metzinger L, Watt DJ, Dickson JG, Tinsley JM, and Davies KE. Utrophin-dystrophin-deficient mice as a model for Duchenne muscular dystrophy. Cell 90: 717-727, 1997.
7. Deconinck N, Tinsley J, De Backer F, Fisher R, Kahn D, Phelps S, Davies K, and Gillis J-M. Expression of truncated utrophin leads to major functional improvements in dystrophin-deficient muscles of mice. Nat Med 3: 1216-1221, 1997.
8. Dixon AK, Tait T-M, Campbell EA, Bobrow M, Roberts RG, and Freeman TC. Expression of the dystrophin-related protein 2 (Drp2) transcript in the mouse. J Mol Biol 270: 551-558, 1997.
9. Dupont-Versteegden EE and McCarter RJ. Differential expression of muscular dystrophy in diaphragm versus hindlimb muscles of mdx mice. Muscle Nerve 15: 1105-1110, 1992.

10. Gilliland G, Perrin S, Blanchard K, and Bunn HF. Analysis of cytokine mRNA and DNA: Detection and quantitation by competitive polymerase chain reaction. Proc Natl Acad Sci USA 87: 2725-2729, 1990.

11. Gillis JM. The mdx mouse diaphragm: Exercise-induced injury (a reply). Muscle Nerve 20: 394, 1997.

12. Hawke TJ and Garry DJ. Myogenic satellite cells: physiology to molecular biology. J Appl Physiol 91: 534-551, 2001.

13. Hill M and Goldspink G. Expression and splicing of the insulin-like growth factor gene in rodent muscle is associated with muscle satellite (stem) cell activation following local tissue damage. J Physiol 549: 409-418, 2003.

14. Irintchev A, Zeschnigk M, Starzinski-Powitz A, and Wernig A. Expression pattern of M-cadherin in normal, denervated, and regenerating mouse muscles. Dev Dyn 199: 326-337, 1994.

15. Muller J, Vayssiere N, Royuela M, Leger ME, Muller A, Bacou F, Pons F, Hugon G, and Mornet D. Comparative evolution of muscular dystrophy in diaphragm, gastrocnemius and masseter muscles from old male mdx mice. J Muscle Res Cell Motil 22: 133-139, 2001.

16. Noden DM, Marcucio R, Borycki A-G, and Emerson CP Jr. Differentiation of avian craniofacial muscles: I. Patterns of early regulatory gene expression and myosin heavy chain synthesis. Dev Dyn 216: 96-112, 1999.

17. Ohnuki Y, Saeki Y, Yamane A, and Yanagisawa K. Quantitative changes in the mRNA for contractile proteins and metabolic enzymes in masseter muscle of bite-opened rats. Archs Oral Biol 45: 1025-1032, 2000.

18. Padilla F, Marc Mege R, Sobel A, and Nicolet M. Upregulation and redistribution of cadherins reveal specific glial and muscle cell phenotypes during wallerian degeneration and muscle denervation in the mouse. J Neurosci Res 58: 270-283, 1999.

19. De la Porte S, Morin S, and Koenig J. Characteristics of skeletal muscle in mdx mutant mice. Int Rev Cytol 191: 99-148, 1999.

20. Porter JD, Rafael JA, Ragusa RJ, Brueckner JK, Trickett JI, and Davies KE. The sparing of extraocular muscle in dystrophinopathy is lost in mice lacking utrophin and dystrophin. J Cell Sci 111 (Pt 13): 1801-1811, 1998.

21. Reimann J, Irintchev A, and Wernig A. Regenerative capacity and the number of satellite cells in soleus muscles of normal and mdx mice. Neuromuscul Disord 10: 276-282, 2000.

22. Rybakova IN, Patel JR, Davies KE, Yurchenco PD, and Ervasti JM. Utrophin binds laterally along actin filaments and can couple costameric actin with sarcolemma when overexpressed in dystrophin-deficient muscle. Mol Biol Cell 13: 1512-1521, 2002.

23. Sabourin LA and Rudnicki MA. The molecular regulation of myogenesis. Clin Genet 57: 16-25, 2000.

24. Seale P, Sabourin LA, Girgis-Gabardo A, Mansouri A, Gruss P, and Rudnicki MA. Pax7 is required for the specification of myogenic satellite cells. Cell 102: 777-786, 2000.

25. Siebert PD and Larrick JW. Competitive PCR. Nature 359: 557-558, 1992.

26. Soussi-Yanicostas N, Barbet JP, Laurent-Winter C, Barton P, and Butler-Browne GS. Transition of myosin isozymes during development of human masseter muscle. Persistence of developmental isoforms during postnatal stage. Development 108: 239-249, 1990.

27. Stedman HH, Sweeney HL, Shrager JB, Maguire HC, Panettieri RA, Petrof B, Narusawa M, Leferovich JM, Sladky JT, and Kelly AM. The mdx mouse diaphragm reproduces the degenerative changes of Duchenne muscular dystrophy. Nature 352: 536-539, 1991.

28. Tajbakhsh S, Rocancourt D, Cossu G, and Buckingham M. Redefining the genetic hierarchies controlling skeletal myogenesis: Pax-3 and myf-5 act upstream of MyoD. Cell 89: 127-138, 1997.

29. Tiffin N, Williams RD, Shipley J, and Pritchard-Jones K. PAX7 expression in embryonal rhabdomyosarcoma suggests an origin in muscle satellite cells. Br J Cancer 89: 327-332, 2003.

30. Tinsley J, Deconinck N, Fisher R, Kahn D, Phelps S, Gillis J-M, and Davies K. Expression of full-length utrophin prevents muscular dystrophy in mdx mice. Nat Med 4: 1441-1444, 1998.

31. Urushiyama T, Akutsu S, Miyazaki J-I, Fukui T, Diekwisch TGH, and Yamane A. Change from a hard to soft diet alters the expression of insulin-like growth factors, their receptors, and binding proteins in association with atrophy in adult mouse masseter muscle. Cell Tissue Res 315: 97-105, 2004.

32. Wachtler F and Christ B. The basic embryology of skeletal muscle formation in vertebrates: the avian model. Semin Dev Biol 3: 217-227, 1992.

33. Weir AP, Burton EA, Harrod G, and Davies KE. A- and B-utrophin have different expression patterns and are differentially up-regulated in mdx muscle. J Biol Chem 277: 45285-45290, 2002.

34. Yamane A, Mayo M, Shuler C, Crowe D, Ohnuki Y, Dalrymple K, and Saeki Y. Expression of myogenic regulatory factors during the development of mouse tongue striated muscle. Archs Oral Biol 45: 71-78, 2000.

35. Yamane A, Mayo ML, and Shuler C. The expression of insulin-like growth factor-I, II and their cognate receptor 1 and 2 during mouse tongue embryonic and neonatal development. Zool Sci 17: 935-945, 2000.

36. Yamane A, Takahashi K, Mayo M, Vo H, Shum L, Zeichner-David M, and Slavkin HC. Induced expression of MyoD, myogenin and desmin during myoblast differentiation in embryonic mouse tongue development. Archs Oral Biol 43: 407-416, 1998.

Figure legends

Fig.1. (A) Electrophoretic gel pattern of the m-cadherin and its competitor after competitive PCR to examine the relation between the amount of PCR products and the concentration of the m-cadherin cDNA. The target gene is shown in the upper bands, while the competitor is shown in the lower band.

(B) The regression line for the m-cadherin generated from the result of image analysis of the electrophoretic bands in (A). The formula of the regression line is $y = 0.772x + 0.978$, where y is the logarithmic value of the ratio of the fluorescent intensity in the m-cadherin band to that in its competitor band, and x is the logarithmic value of the concentration of the m-cadherin cDNA.

Fig. 2. (A ~ D) Hematoxylin and eosin staining images of the masseter (A), gastrocnemius (B), soleus (C), and diaphragm (D) muscles of mdx mice.

(E) The area of the degenerative region is shown relative to the total muscle area of the mdx mice. Each column and vertical bar represent the mean + 1 SD of six mdx mice. The vertical axis is expressed as a percentage of the total sectional area of the muscles set at 100. Significant differences among the mdx muscles, $^{\varphi\varphi}p<0.01$, $^{\varphi\varphi\varphi}p<0.001$.

Fig. 3. (A) Typical example of gel electrophoretic pattern for pax7 competitive RT-PCR products of the masseter, gastrocnemius, soleus, and diaphragm muscles obtained from control C57BL/10J (B10) and mdx mice. The target gene is shown in the lower bands, while the competitor is shown in the upper band.

(B) The mRNA expression levels for pax7 in the masseter, gastrocnemius, soleus, and diaphragm muscles obtained from control B10 and mdx mice. Each column and vertical bar

represent the mean + 1 SD of six B10 or mdx mice. The vertical axis is expressed as a percentage of the mean value of the B10 masseter muscle set at 100. Significant differences between the B10 and mdx mice, *$p<0.05$, **$p<0.01$. Significant difference among the mdx muscles, $^{\varphi\varphi}p<0.01$.

(C) A scatter diagram and a regression line between the degenerative areas of the skeletal muscles and the expression levels for pax7 in the mdx mice.

Fig. 4. (A) The mRNA expression levels for m-cadherin in the masseter, gastrocnemius, soleus, and diaphragm muscles obtained from control C57BL/10J (B10) and mdx mice. Each column and vertical bar represent the mean + 1 SD of six B10 or mdx mice. The vertical axis is expressed as a percentage of the mean value of the B10 masseter muscle set at 100.

(B, C, D) Immunostaining images for m-cadherin in the mdx masseter muscle tissues. Arrows in B and C indicate the satellite cells identified by immunostaining for m-cadherin. Arrows in D indicate the m-cadherin-positive cells in the area interspaced among the myofibers.

(E) The percentage of satellite cells to the total number of cell nuclei in the masseter, gastrocnemius, soleus, and diaphragm muscles obtained from control C57BL/10J (B10) and mdx mice. Each column and vertical bar represent the mean + 1 SD of six B10 or mdx mice. Significant differences between the B10 and mdx muscles, *$p<0.05$, **$p<0.01$, ***$p<0.001$. Significant difference among the mdx muscles, $^{\varphi\varphi}p<0.01$.

(F) A scatter diagram and a regression line between the degenerative areas of the skeletal muscles and the percentages of satellite cells to the total number of cell nuclei in the muscle tissues in the mdx mice.

Fig. 5. (A) The mRNA expression levels for utrophin in the masseter, gastrocnemius, and diaphragm muscles obtained from control C57BL/10J (B10) and mdx mice. Each column and

vertical bar represent the mean + 1 SD of six B10 or mdx mice. The vertical axis is expressed as a percentage of the mean value of the B10 masseter muscle set at 100. Significant differences between the B10 and mdx muscles, *$p<0.05$, ***$p<0.001$. Significant differences among the mdx muscles, $^{\varphi}p<0.05$, $^{\varphi\varphi}p<0.01$.

(B) A scatter diagram and a regression line between the degenerative areas of the skeletal muscles and the expression levels for utrophin mRNA in the mdx mice.

(C~F) Immunostaining images for utrophin in the masseter (C, D) and diaphragm (E, F) muscle tissues of the B10 (C, E) and mdx (D, F) mice. Black and white arrowheads in C, D, E, and F indicate the immunostaining for utrophin in the periphery of the myofibers. Arrows in D indicate the sarcoplasm of normal myofibers unstained for utrophin. E is the same magnification at C. F is the same magnification at D.

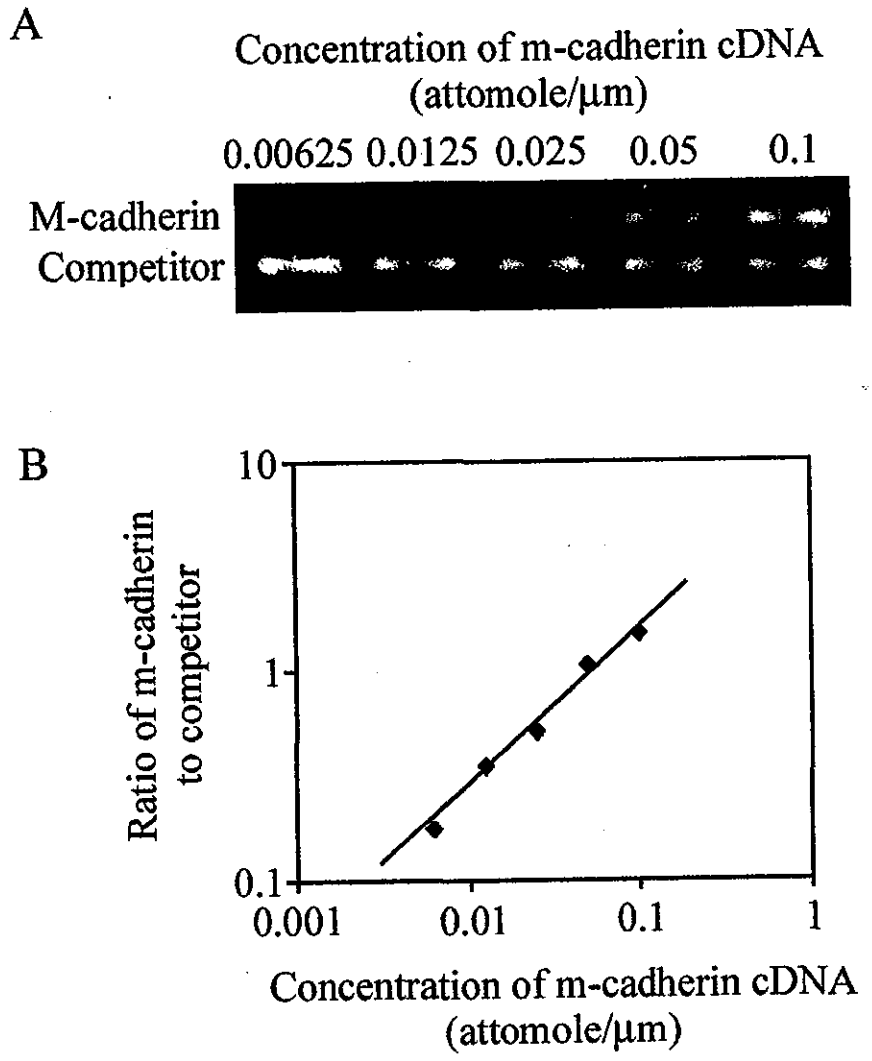
A
Concentration of m-cadherin cDNA
(attomole/μm)
0.00625 0.0125 0.025 0.05 0.1
M-cadherin
Competitor
B
Ratio of m-cadherin
to competitor
10
1
0.1
0.001
0.01
0.1
1
Concentration of m-cadherin cDNA
(attomole/μm)

Fig. 1

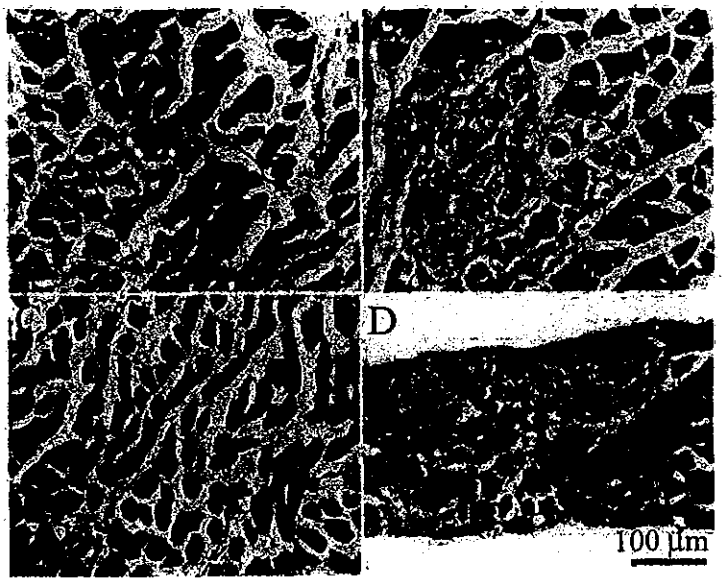
D
100 μm

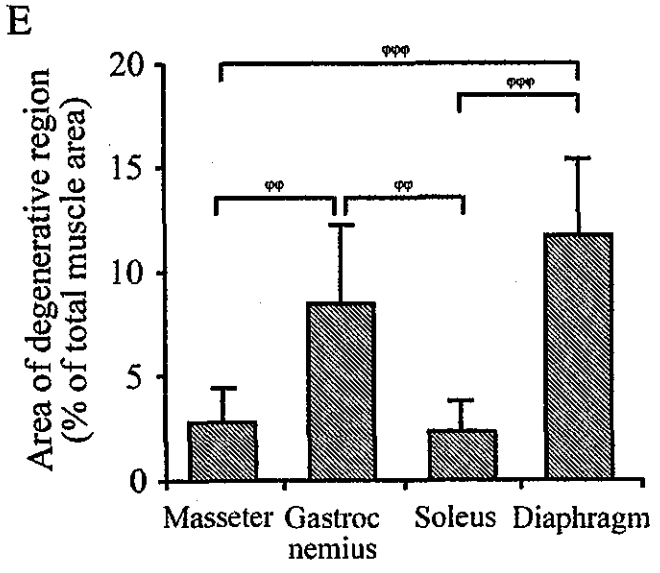
E
Area of degenerative region
(% of total muscle area)
20
15
10
5
0
φφφ
φφφ
φφ
φφ
Masseter
Gastroc
nemius
Soleus
Diaphragm

Fig. 2

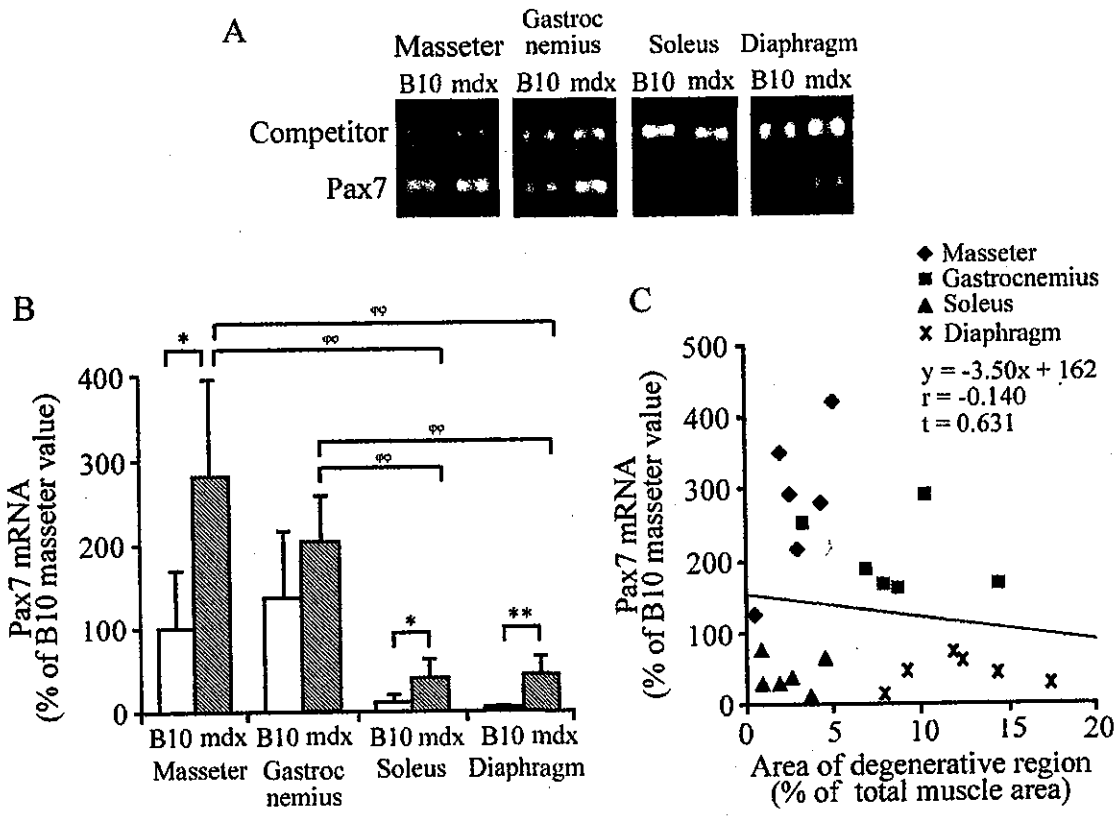
A
Masseter
Gastroc nemius
Soleus
Diaphragm
B10 mdx
Competitor
Pax7
B
Pax7 mRNA (% of B10 masseter value)
400
300
200
100
0
B10 mdx
Masseter
Gastroc nemius
Soleus
Diaphragm
C
Masseter
Gastrocnemius
Soleus
Diaphragm
y = -3.50x + 162
r = -0.140
t = 0.631
500
400
300
200
100
0
5
10
15
20
Area of degenerative region (% of total muscle area)

Fig. 3